FORMATION MECHANISM OF SILICA SCALE IN DIENG GEOTHERMAL POWER PLANT, INDONESIA

Saefudin Juhri^{1,2}, Kotaro Yonezu¹, Takushi Yokoyama^{1,3}, M Istiawan Nurpratama⁴, Agung Harijoko²

Department of Earth Resources Engineering, Kyushu University, 744 Motooka, Nishi-ku, Fukuoka 819-0395, JAPAN

⁴ PT Geo Dipa Energi unit Dieng, Dieng Kulon, Batur, Banjarnegara 53456, INDONESIA

juhri@mine.kyushu-u.ac.jp

Keywords: polymerization, silica scale, iron, Dieng

ABSTRACT

Severe silica scale problem has occurred in Dieng geothermal power plant since the start of its operation. Silica scale is formed in surface pipeline systems, and this requires acidification of the brine using sulfuric acid to address the problem. In order to understand the formation mechanism of silica scale inside the brine pipeline, the polymerization behavior of silicic acid in geothermal water, and the precipitation of scale and its characteristics, were investigated in an on-site batch experiment.

The polymerization of silicic acid was investigated by spectrophotometry to determine monosilicic acid (SiO₂(M)) and by ICP-OES to determine total silicic acid (SiO₂(T)). Under neutral pH condition, SiO₂(M) concentration decreased rapidly from 1,000 to 350 ppm, while SiO₂(T) decreased moderately from 1,000 to 350 ppm. This suggests that silica precipitation follows the rapid growth of polysilicic acid. Even under acidic pH condition, polymerization proceeds: SiO₂(M) concentration decreased from 1,000 to 600 ppm. However, SiO₂(T) concentration was kept almost constant. This suggests that addition of sulfuric acid was not able to completely stop the polymerization of monosilicic acid, but only retarded the growth of particles (reaction between polysilicic acids).

Trace metal concentrations such as iron (Fe) and/or aluminum (Al), reported to promote the formation of silica scale, were determined by ICP-OES. Under neutral pH condition, a decrease in Fe concentration was observed coinciding with the decreasing $SiO_2(T)$ concentration. This suggests that Fe concentration in the brine is playing a role in the deposition of silica under neutral pH condition by accelerating the growth of polysilicic acids. On the other hand, both the Fe and $SiO_2(T)$ concentration in the brine remained constant after acidification by sulfuric acid. This suggests that Fe ions were prevented from binding into the polysilicic acid under acidic condition. Furthermore, the XRD and XRF analyses show that the scale is mainly composed of amorphous silica with high concentration of Fe.

1. INTRODUCTION

Severe silica scaling problem has occurred in Dieng geothermal power plant since the beginning of its operation in 2002. With initial capacity of 60 MW, this power plant is operated by PT Geo Dipa Energi. An expansion is planned to increase the electric capacity, yet the company still struggles with silica scaling problem.

The power plant is supplied by several production wells. Some of them produce mainly steam, two-phase, and water. This study, however, only focus on a two-phase production well which supplies fluid to a separation system and brine pipeline where severe silica scale problem was encountered. Brine water discharged from this production well is a hypersaline geothermal water which contains more than 3.5% wt total salt concentration and silica (SiO₂) of 1,000 ppm. Iron (Fe) appears in relatively low concentration of 1.35 ppm, however due to flashing process at air-flasher tank, the concentration increases up to 2 ppm at open canal system. The chemistry of the geothermal fluid collected from production well is shown in Table 1.

Table 1: Chemical characteristic of Dieng geothermal water collected from brine-dominated production well.

	Unit	
Cl	ppm	21200
SO ₄		74.4
HCO ₃		25.0
Na		10249
K		2817
Ca		709
Mg		0.5
SiO ₂		1065
Al		0.01
Fe		1.35

The wellpad consists of one production well with two separators due to high productivity of this production well (Figure 1). Brine water from separators flows through two different brine pipes to two air-flasher tanks. Water discharged from air-flasher tanks finally mixed at open canal and pond system before enters reinjection pipeline, and pumped to reinjection well. In order to overcome silica scaling problem, sulfuric acid is dosed into the brine pipelines to prevent the formation of silica scale inside the brine pipes. Meanwhile, open canal and pond system is employed to prevent formation of silica scale inside reinjection pipeline by decreasing temperature of geothermal water to let silica precipitate along the canal and pond. However, the effectivity of the canal and pond is decreased due to acidification at brine pipe.

In this study, polymerization experiment was conducted to understand the formation of silica scale inside the brine pipelines between the separator and air-flasher tanks. The polymerization experiment was conducted at two brine pH conditions: before acidification (near neutral pH) and after

² Department of Geological Engineering, Universitas Gadjah Mada, Sinduadi, Mlati, Sleman 55284, INDONESIA

³ Geothermal Division, West Japan Engineering Consultant, 111 Watanabe Dori, Chuo-ku, Fukuoka 810-0004, JAPAN

acidification (around pH 5). This was done to understand the formation mechanism of silica scale inside brine pipe under both pH condition, the mechanism of sulfuric acid in preventing the formation of silica scale and the role of Fe in the formation of the scale. In addition, adsorption experiments using silica gels (i.e. D-50-1000AW and Mallinckrodt) were also conducted at two brine pH conditions to investigate the interaction between silicic acid in geothermal water with existing silica scale (represented by silica gel).

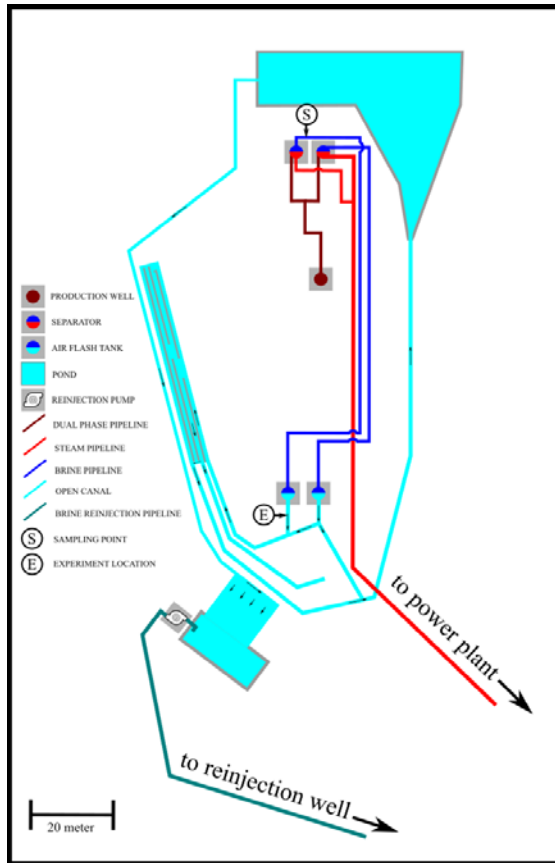


Figure 1: The sketch of wellpad of the study area.

2. METHODS

2.1 Experimental procedure

In order to study the polymerization behavior and deposition of silicic acid in Dieng geothermal water, one liter of geothermal water was taken from the sampling point at brine pipe just after the separator (Figure 1). The pH condition was controlled by stopping sulfuric acid injection (neutral pH: 6.57 - 6.60) and continuing injection (acidified pH: 5.10 -5.31). The geothermal water taken from sampling point was put in one liter polypropylene bottle as reaction vessel which then put in flowing geothermal water at open canal to maintain high temperature (80 - 90 °C). The polymerization experiment was conducted for one hour where 50 mL of geothermal water was taken from the reaction vessel at each designated reaction time. The collected samples were filtered with 0.45 µm membrane filter and acidified with 0.1 M nitric acid to prevent further polymerization prior to the following analysis. To characterize the silica scale found in the brine pipeline, a scale was collected for X-ray diffraction (XRD) and X-ray fluorescence (XRF) spectroscopy analysis.

The adsorption experiments using silica gels were conducted following the same procedure as described above, with 0.8

grams of silica gel were added into 800 mL of geothermal water keeping ratio of 1 gram/Liter silica gel. Two types of silica gel were examined: D-50-100AW and Malinckrodt. These experiments were conducted for 30 minutes. Solution samples collected from this experiment were analyzed through spectrophotometry and ICP-OES analysis. The change in concentrations of SiO₂(T) and total Fe concentration were monitored to understand the effect of silica gel in the deposition of silicic acid in geothermal water.

2.2 Analytical methods

Spectrophotometry analysis was conducted onsite to determine the monosilicic acid in geothermal water (SiO₂ (M)). Geothermal water was diluted and mixed with 0.1 M hydrochloric acid and 5 wt% of molybdate. The molybdosilicic acid showed yellowish color which then analyzed using HACH DR-1900. The absorbance value obtained from the analysis was calculated to get concentration of SiO₂ (M). Meanwhile, total silicic acid concentration (SiO₂ (T)) was obtained through inductively coupled plasma – optical emission spectroscopy (ICP-OES) analysis using Perkin-Elmer Optima 5300DV in Economic Geology Laboratory, Kyushu University.

As for silica scale sample collected from brine pipe, XRD analysis was carried out using Rigaku UltimaIV while XRF analysis was conducted using Rigaku RIX3100 instrument. The sample was rinsed by ultrapure water and air dried prior to each analysis, and further dried by oven at 50°C for 24 hours prior to XRF analysis.

3. RESULT

3.1 Change of silicic acid and iron

In the polymerization experiment under neutral pH condition, the SiO₂(M) concentration was observed to decrease rapidly from 923 to 350ppm during the first 15 minutes of the experiment (Figure 2). This suggests rapid polymerization of silicic acid, which then gradually slowed down (from 350 to 346ppm) in the next 45 minutes as the SiO₂(M) concentration reached the solubility of amorphous silica at 80 °C. The SiO₂(T) concentration also decreased gradually (from 971 to 865ppm) in the first 15 minutes (induction period), then rapidly decreased from 865 to 349 ppm between 15-30 minutes (precipitation period) until it reached the concentration of SiO₂(M) (around 350 ppm) beyond 30 minutes. The Fe concentration also dropped consistent with the drop in SiO₂(T) concentration, from an initial 1.78 to 1.52ppm in 15 minutes, and then rapidly decreased to 0 ppm after 30 minutes.

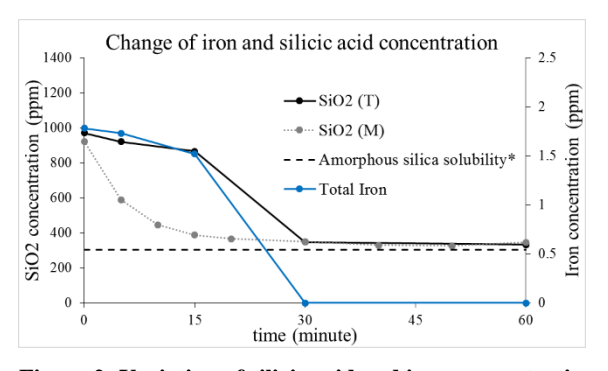


Figure 2: Variation of silicic acid and iron concentration in geothermal water during polymerization experiment under neutral pH condition (*according to Marshall, 1980).

On the other hand, decrease in $SiO_2(M)$ concentration was observed to be much slower under the acidified pH condition, from an initial 1,023 to 630ppm at the end of the experiment (Figure 3). The $SiO_2(T)$ concentration also decreased only slightly from 1,016 to 926ppm. Similarly, the Fe concentration has not changed significantly and remained at around 1.8 ppm during the experiment.

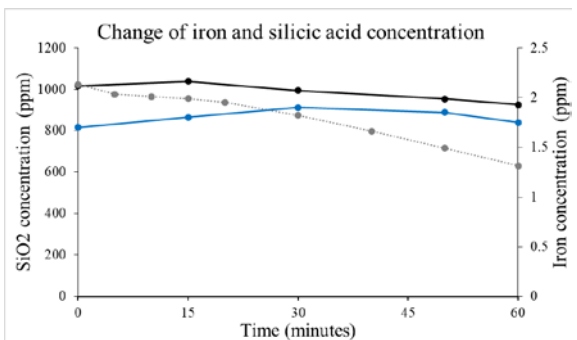


Figure 3: Change of silicic acid and iron concentration in geothermal water during polymerization experiment under acidified pH condition.

For the adsorption experiments under neutral pH condition, the changes in $SiO_2(M)$ concentration were similar to that in the previous polymerization experiments at same condition. With the addition of D-50-1000AW and Mallinckrodt silica gel, $SiO_2(M)$ concentration decreased from 923 to 348ppm (Figure 4) and from 923 to 345ppm (Figure 5), respectively. Likewise, the $SiO_2(T)$ concentration also decreased at the similar rate as the polymerization experiment: from 971 to 377ppm in D-50-1000AW adsorption experiment and from 971 to 475ppm in Mallinckrodt adsorption experiment. The Fe concentration also decreased during both adsorption experiments from 1.78 to 0.05 ppm and from 1.78 to 0.33 ppm, respectively.

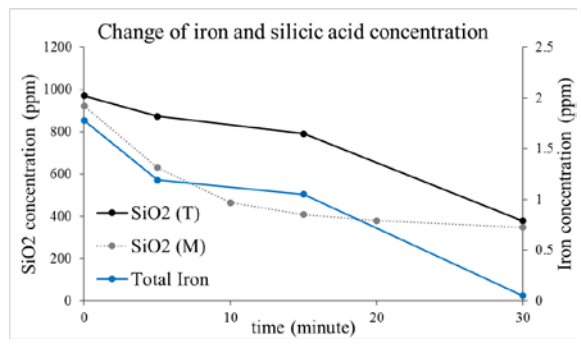


Figure 4: Change of silicic acid and iron concentration in geothermal water during D-50-1000AW silica gel adsorption experiment under neutral pH.

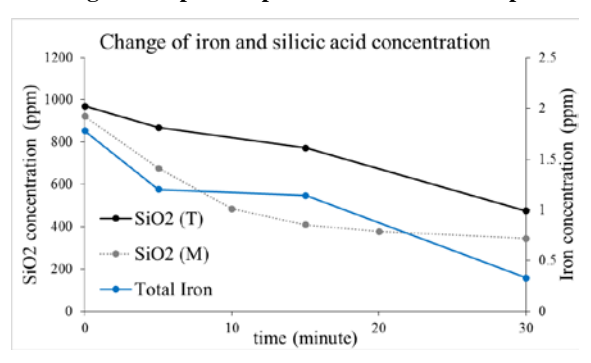


Figure 5: Change of silicic acid and iron concentration in geothermal water during Mallinckrodt silica gel adsorption experiment under neutral pH.

For the adsorption experiments under acidified condition (Figures 6 and 7), a change in the chemical trends were observed. The total silicic acid $SiO_2(T)$ concentration decreased more rapidly in the adsorption experiment compared to that in the polymerization experiments in the first 30 minutes. The $SiO_2(T)$ decreased from 1,016 to 952ppm during D-50-1000AW silica gel adsorption experiment (Figure 6), while it decreased from 1,016 to 995ppm during polymerization experiment (Figure 3). The $SiO_2(T)$ concentration decreased even more rapidly during Mallickrodt silica gel adsorption experiment, from 1,016 to 758ppm (Figure 7). However, the Fe concentration remained at high level during both adsorption experiments (around 1.7 ppm) under acidified pH condition.

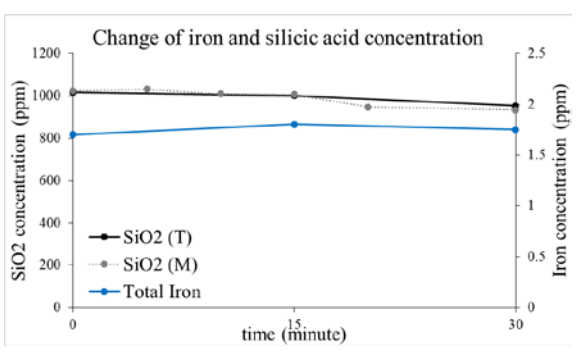


Figure 6: Change of silicic acid and iron concentration in geothermal water during D-50-1000AW silica gel adsorption experiment under acidified pH.

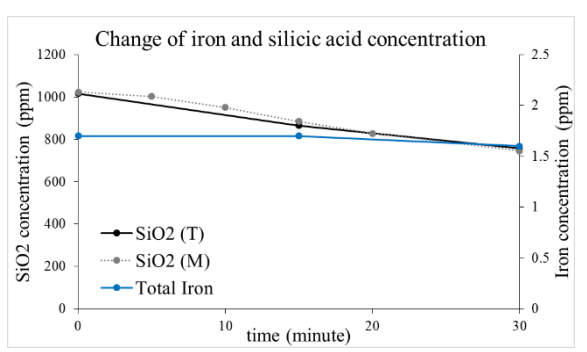


Figure 7: Change of silicic acid and iron concentration in geothermal water during Mallinckrodt silica gel adsorption experiment under acidified pH.

3.2 XRD pattern

The XRD patterns (Figure 8) show that the scale collected from the brine pipe is composed mainly of amorphous silica as indicated by a scattering pattern at 2theta = $22-23^{\circ}$ (Manceau et al., 1995). Furthermore, some quite distinct peaks could be detected at 2theta = 30.04° and 43.04° (or d spacing = 2.970 Å and 2.099 Å, respectively) which can be regarded as galena (PbS). The peaks at 2theta = 35.40° , 56.89° , and 62.50° (or d spacing = 2.533 Å, 1.615 Å, and 1.485 Å, respectively) can be regarded as magnetite (Fe₃O₄).

3.3 XRF result

The chemical characteristics of the silica scale is presented in Table 2. The main component of the scale is SiO₂ which account for 90.01 wt%, followed by FeO (1.91 wt%) and Al₂O₃ (0.74 wt%). The scale sample is believed to be formed within a year of production which mostly under acidified

condition at pH=5. In addition, the lead (Pb) content reached 0.19 wt%, while sulfur (S) is 0.17 wt%. The chemical composition data is consistent with mineralogical data. Galena (PbS) shows quite strong peaks by XRD pattern.

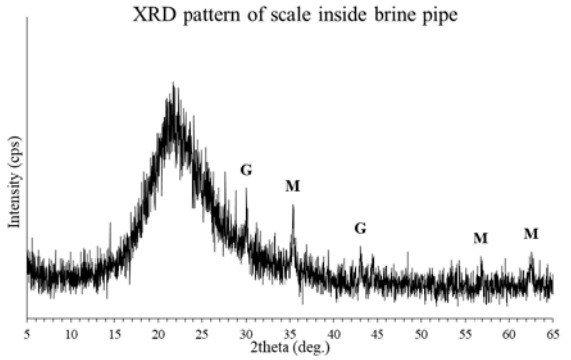


Figure 8: XRD pattern of silica scale sample collected from brine pipe (G = galena, M = magnetite).

Table 2: XRF analysis result of silica scale sample collected from brine pipe.

Amount (wt %)		
90.01		
n.d.		
0.74		
1.91		
0.04		
0.30		
0.16		
0.48		
0.35		
n.d.		
5.58		
0.17		
0.02		
0.04		
0.20		

4. DISCUSSION

4.1 Polymerization and precipitation mechanism, and effect of acidification

The first 15 minutes of the polymerization experiment under neutral pH condition indicated rapid interaction of SiO₂(M) or M-M reaction (Tarutani, 1989) to form polysilicic acid (SiO₂(P)) (see Figure 2). During this period, less silicic acid was deposited as M-M reaction involving monosilicic acids dominate rather than polysilicic acids (P-P reaction). However, in the next 15 minutes, most SiO₂(M) had been polymerized into SiO₂(P), with P-P reaction happening rapidly during this period to form larger polysilicic acid having molecular size of $\sim >450$ nm. As the larger polysilicic acid particles could not pass through the filter membrane these were deposited on the filter. In the last 30 minutes of the experiment, SiO₂(M) concentration in geothermal water already reached the solubility of amorphous silica at the presence of 0.6 molar salt (calculation according to Marshall, 1980). During this period, both M-M and P-P reactions were significantly slowed down. Furthermore, the drop in Fe concentration that coincided with the decreasing SiO₂(T) concentration seems to suggest that both are deposited at the same time (between 15-30 minutes).

The importance of Fe in the polymerization and deposition of silicic acid in Dieng geothermal water has been studied by several researchers (e.g. Gallup and Reiff, 1991; Manceau et al., 1995; and Yokoyama et al., 1993). It is believed that Fe is incorporated in the polymerization of silicic acid as $Fe(OH)_3$, , as evidenced by the change in both the Fe and SiO2 concentrations in Dieng geothermal water. On the other hand, both Fe and $SiO_2(T)$ concentration remained at high levels during the polymerization experiment under acidified condition, with polymerization occurring a much slower rate.

To understand the mechanism of silicic acid precipitation, a geochemical model was constructed based on the actual chemical composition of Dieng geothermal water. Water samples are collected from two-phase pipe (before separator) and brine pipe (after separator). The redox condition is based on the knowledge of previous studies (e.g. Gallup, 1993 and McKibben and Eldridge, 1989) and is set to be from -500 mV to 1,000 mV, while pH is set to be from 3.0 to 9.0. Some minerals need to be suppressed from the model due to incompatible thermodynamic condition. Minerals included in the model are based on the previously found in geothermal scale (especially in Fe rich, high salinity, and high silica content geothermal water) such as amorphous silica, arsenopyrite, chalcopyrite, calcite, cronstedtite, $Fe(OH)_2(ppd)$, $Fe(OH)_3(ppd)$, $Fe_2(SO_4)_3(C)$, goethite, hematite, magnetite, nontronite-(Ca/K/Mg/Na), epidote, pyrite, and pyrrhotite (from McKibben and Williams, 1989; Gallup and Reiff, 1991; Gallup, 1993; Yokoyama et al, 1993; Manceau et al, 1995; Eggleton and Tilley, 1998).

The speciation of Fe is essential in this study. Gunnlaugsson and Arnorsson (1982) has investigated the speciation of iron in geothermal water and concluded that below 150 °C iron exists predominantly as Fe^{2+} (ferrous iron), while at higher temperature $Fe(OH)_4$ (ferric iron) is the dominant species from the dissolution of iron-bearing minerals such as pyrite, marcasite, and pyrrhotite. Furthermore, MacKibben and Williams (1989) studied the speciation of Fe in high salinity geothermal water. Their study showed that Fe^{2+}/Fe^{3+} ratio increase by the increase of salinity, where both can co-exist as chloride salts. Preliminary model of Fe speciation suggests the co-existence of ferrous iron as $FeCl^+$ and ferric iron as $Fe(OH)_2^+$.

In the presence of Fe³⁺ as Fe(OH)₂⁺ in geothermal water, stability of silica is highly controlled by Fe-Si-OH complex (see Figure 9). In this model, temperature and pressure were set to brine pipe's temperature (180°C) and pressure (8-10 bars). This model support the idea of Fe interaction with SiO₂ in the precipitation of silicic acid in Dieng geothermal water. Yokoyama et al. (1980) suggested that ferrous hydroxide adsorbs monosilicic acid in geothermal water on which monosilicic acid polymerized to form polysilicic acid and further degree of polymerization. The study mentioned that this interaction occurred most rapidly under pH 9 while it decreases by decreasing the pH.

An on-site spectrophotometric analysis was conducted to determine the occurrence of ferric iron in geothermal water by the addition of ferron (7-iodo-8-hydroxyquinoline-5-sulphonic acid) and pH adjustment to 5. The result (Figure 10) suggests that iron predominantly exists as ferric iron in Dieng geothermal water at initial condition. During polymerization experiment under neutral pH condition, the concentration of ferric hydroxide decreases with time consistent with the decreasing monosilicic acid concentration. This suggests that ferric hydroxide is

incorporated into polysilicic acid during the early stage of polymerization. The result is in agreement with the thermodynamic model that silica stability is likely controlled by iron concentration in the brine.

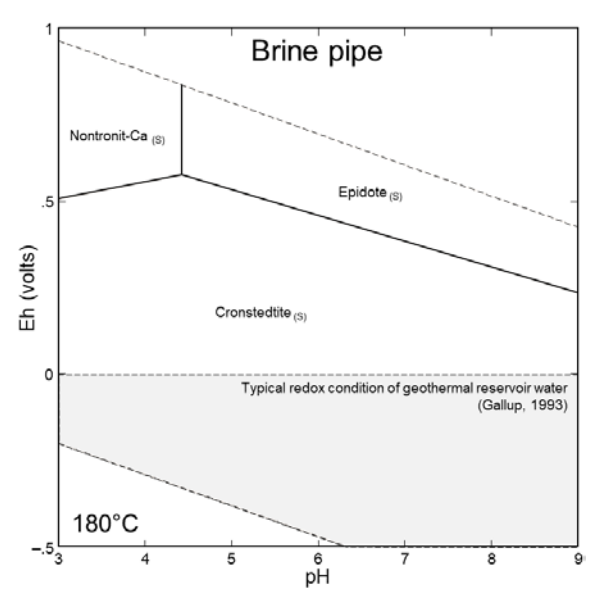


Figure 9: Eh-pH diagram of the stability of SiO₂ in Dieng geothermal water.

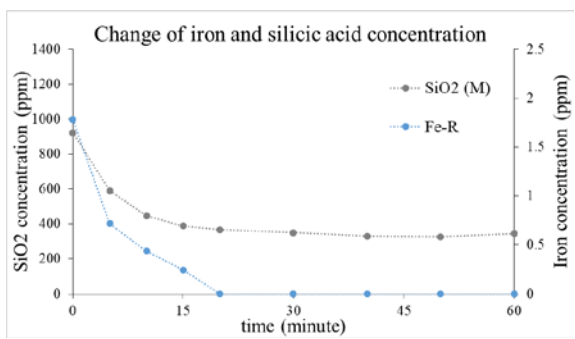


Figure 10: Change of monosilicic acid and ferronreactive iron (ferric hydroxide) during polymerization experiment under neutral pH condition.

In addition, due to limited amount of Fe in geothermal water, these Fe-Si-OH complex minerals might not be detected by XRD. Furthermore, after all Fe in geothermal water was removed, the stability of SiO_2 might change to amorphous silica or quartz, where quartz is more unlikely according to Weres et al (1980) and observation of chemical change in polymerization experiment.

4.1 Effect of the presence of silica scale

Adsorption experiment by D-50-1000AW and Mallinckrodt silica gel simulated the effect of existing silica scale inside the brine pipe to the precipitation of silicic acid in geothermal water. There was not a significant change in the polymerization and precipitation of silicic acid under neutral pH due to rapid rate of polymerization and growth of polysilicic acid. On the other hand, the effect of silica gel can be observed under acidified pH condition where the addition of Mallinckrodt somewhat accelerates the drop in total silicic acid concentration.

Both SiO₂(M) and SiO₂(T) decreased simultaneously during the experiment (Figure 10) which resembles the adsorption of silicic acid onto the silica gel surface. The adsorption of silicic acid on silica gel is much faster than the rate of polymerization of monosilicic acid, which suggest that interaction between monosilicic acid and silica gel is more favorable than reaction among monosilicic acids.

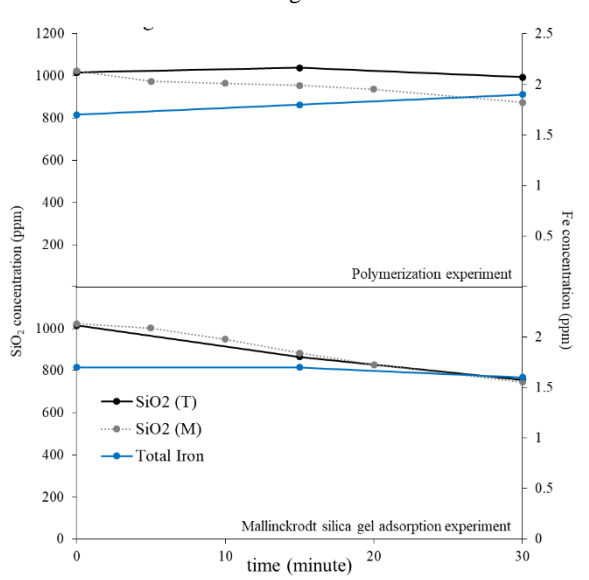


Figure 10: Change of silicic acid and iron concentration in geothermal water during polymerization and adsorption experiments.

In addition, the Fe concentration did not change significantly by this time, and imply that Fe was not incorporated in the interaction between $SiO_2(M)$ and silica gel. The interaction between $SiO_2(M)$ and silica gel indicated that monosilicic acid particles in Dieng geothermal water are depositing on the surface of existing silica scale inside the pipeline. Moreover, the comparison of the result from the adsorption experiment with XRD analysis of the scale, is suggesting that under operational condition (acidified pH) silica scale can still form as amorphous silica without higher degree of polymerization or Fe incorporation.

5. CONCLUSION

The silica scale formed in Dieng geothermal power plant consisted mainly of SiO₂ followed by high concentration of Fe and Al. The contribution of Fe in the polymerization and precipitation of silica is investigated and confirmed. Under neutral pH condition, the Fe and SiO₂ precipitate simultaneously from geothermal water, while after acidification, the concentrations of both Fe and SiO₂ remained relatively high. The addition of sulfuric acid to lower the brine pH successfully slowed down the rate of polymerization and precipitation of silicic acid. Through adsorption experiment we found that monosilicic acid can still attach on the surface of silica gel (representing silica scale in pipeline) under acidified condition even without polymerization or incorporation of Fe.

ACKNOWLEDGEMENTS

We would like to thank JICA (Japan International Cooperation Agency) for the financial support in this research.

REFERENCES

Eggleton, R.A. and Tilley, D.B. Hisingerite: A Ferric Kaolin Mineral with Curved Morphology. Clays and Clay Minerals, vol. 46, p. 400-413. (1998).

Gallup, D.L. and Reiff, W.M. Characterization of Geothermal Scale Deposits by Fe-57 Mossbauer Spectroscopy and Complementary X-ray Diffraction and Infra-red Studies. Geothermics, vol. 20, no. 4, p. 207-224. (1991).

Gallup, D.L. The Use of Reducing Agents for Control of Ferric Silicate Scale Deposition. Geothermics, Vol. 22, No. 1, pp. 39-48. (1993).

Gunnlaugsson, E. and Arnorsson, S. The Chemistry of Iron in Geothermal Systems in Iceland. Journal of Volcanology and Geothermal Research, vol. 14, p. 281-299. (1982).

Manceau, A., Ildefonse, Ph., Hazemann, J.-L., Flank, A-M., and Gallup, D. Crystal Chemistry of Hydrous Iron Silicate Scale Deposits at the Salton Sea Geothermal Field. Clays and Clay Minerals, vol. 43, no.3, p. 304-317. (1995).

Marshall, W.L. Amorphous silica solubilities-III. Activity coefficient relations and predictions of solubility behavior in salt solutions, 0-350°C. Geochimica et Cosmochimica Acta, vol. 44, p. 925-931. (1980).

McKibben, M.A. and Williams, A.E. Metal Speciation and Solubility in Saline Hydrothermal Fluids: An Empirical Approach Based on Geothermal Brine Data. Economic Geology, vol. 84, p. 1996-2007. (1989).

Tarutani, T. Polymerization of Silicic Acid: A Review. Analytical Science, vol. 5, p. 245-252. (1989).

Weres, O., Yee, A., and Tsao, L. Kinetics of Silica Polymerization. Journal of Colloid and Interface Science, vol. 84, No. 2, pp. 379-402. (1981).

Yokoyama, T., Nakazato, T., and Tarutani, T. Polymerization of Silicic Acid Asorbed on Iron(III) Hydroxide. Bulletin of the Chemical Society of Japan, vol. 53, p. 850-853. (1980).

Yokoyama, T., Sato, Y., Maeda, Y., Tarutani, T., and Itoi, R. Siliceous Deposits Formed from Geothermal Water I. The Major Constituents and the Existing States of Iron and Aluminum. Geochemical Journal, vol. 27, p. 375-384. (1993).